UJEAS

UNIZIK JOURNAL OF ENGINEERING AND APPLIED SCIENCES

UNIZIK Journal of Engineering and Applied Sciences 5(4), December (2025), 2933-2947
Journal homepage: https://journals.unizik.edu.ng/index.php/ujeas
PRINT ISSN: 2992-4383 || ONLINE ISSN: 2992-4391

Enhancing Hydrocarbon prospect delineation through cross-plots and rock physics model: a case study of the NKO field onshore Niger Delta Basin, Nigeria

Ifeanyi Omezi[1], Chukwudi Christopher Ezeh[2]

[1]Department of Petroleum, Nnamdi Azikiwe University, Awka

[2]Department of Geology and Mining, Enugu State University of Science and Technology.

[*]Corresponding Author's E-mail: *i.omezi@unizik.edu.ng*

Abstract
The NKO Field, located in the Central Swamp Depobelt of the Niger Delta Basin, Nigeria, is a structurally complex hydrocarbon-bearing system. This study integrates cross-plot analysis and rock physics modeling to enhance reservoir characterization and hydrocarbon prospect delineation. Well log and seismic data from 32 wells were used to delineate lithofacies, evaluate petrophysical properties, and characterize reservoirs. Results show the reservoirs thin northeastward, with cross-plot analysis effectively distinguishing four fluid/lithology zones: gas, oil, brine, and shale. Rock physics modeling indicates that plastic deformation predominates, causing compaction, reduced porosity and permeability, and impacting hydrocarbon productivity. A petro-elastic model was developed to differentiate reservoir rocks from non-reservoirs, providing insights into elastic and lithological properties. Upscaling of porosity, permeability, net-to-gross, water and hydrocarbon saturation, and facies successfully captured heterogeneity, faults, fractures, and multiphase flow behavior in the reservoirs. A 3D grid-based geological model estimated hydrocarbon volumes: Stock Tank Oil Initially in Place (STOIIP) of ~102.9 million stock tank barrels with a 35% recovery factor, and Stock Tank Gas Initially in Place (STGIIP) of ~1.11 billion stock tank barrels with a 100% recovery factor. These findings demonstrate that integrating cross-plot analysis with rock physics models enhances reservoir evaluation, supports accurate identification of hydrocarbons, and informs optimal field development strategies.

Keywords: Hydrocarbon, cross-plots, rock physics model, NKO field, onshore, Niger Delta Basin

1. Introduction

The NKO field is a complex geological structure with multiple hydrocarbon-bearing reservoirs located within the Central Swamp Depobelt of the Niger Delta in Nigeria. In order to improve exploration and production efficiency, it is important to accurately delineate hydrocarbon prospects and characterize reservoir properties through the integration of cross-plots and rock physics models. Nakajigo et al. (2023) used rock physics analysis of the reservoir units in the Semliki basin, focusing on the Kanywataba well to integrate geophysical and geological data for better reservoir characterization. Cross plots were utilized in confirming conventional trends, revealing that density decreases with porosity while P-wave and S-wave velocities show an increasing trend, indicating the presence of gas and brine sands in the formations. Chris (2022) discussed the application of rock physics models for reservoir characterization, highlighting their potential despite being perceived as complex and reliant on difficult-to-measure parameters. This demonstrated how a simple rock physics model can be effectively calibrated to provide insights into the elastic properties of reservoirs, including porosity, fluid saturation, and mineral composition, as well as net-to-gross ratios.

Triveni and Rima (2021), in their paper, focused on the estimation of petrophysical properties such as effective porosity, volume of shale, and water saturation using well log responses in the Upper Assam basin, India. Rock physics

diagnostic modelling was utilized to predict the elastic properties of rocks, considering factors like fluids, mineral mixtures, and pore textures, with a particular emphasis on the Tipam Sandstone (TS) and Barail Arenaceous Sandstone (BAS) reservoirs. Fast and meaningful evaluation of attributes was enabled by the advancement of Cross-plotting which is a widely used technique in rock physics analysis. (Castagna and Swan, 1997). Pickett (1963) and Goodway et al. (1997) suggested four attributes for lithology and pore fluid discrimination as listed below: Vp/Vs ratio, Lambda modulus and density, Shear rigidity and density, and P-wave Impedance

Allo et al. (2022) investigated the seismic amplitude anomalies in the poorly compacted sandstone reservoirs of the 'Jay' Field, aiming to identify hydrocarbon presence using Amplitude Variation with Angles (AVA) and rock physics techniques. It was revealed that different seismic amplitude reflections are influenced by the fluids and lithologies present, with well logs indicating that some reservoirs are brine-saturated while others contain oil and gas. This study aims to carry out an enhanced hydrocarbon prospect delineation through cross-plots and a rock physics model, which will be achieved through delineating the lithofacies stratigraphic framework using well logs, characterizing the reservoirs, and evaluating their petrophysical properties in the NKO field.

1.1 Location of the study area

The study area is located onshore within the southeastern Central Swamp Depobelt, Niger Delta Basin, Nigeria. It lies between Longitudes 5.8° E and 6.2°E, and Latitudes 5.8° N and 6.1° N (Figure 1.1d). Fifty-seven wells have been drilled in the field to date. Accurate interpretation of well logs is essential for reservoir evaluation and characterization. Log correlation provides the foundation for determining the geometry and architecture of reservoirs, enabling a comprehensive understanding of the subsurface geology.

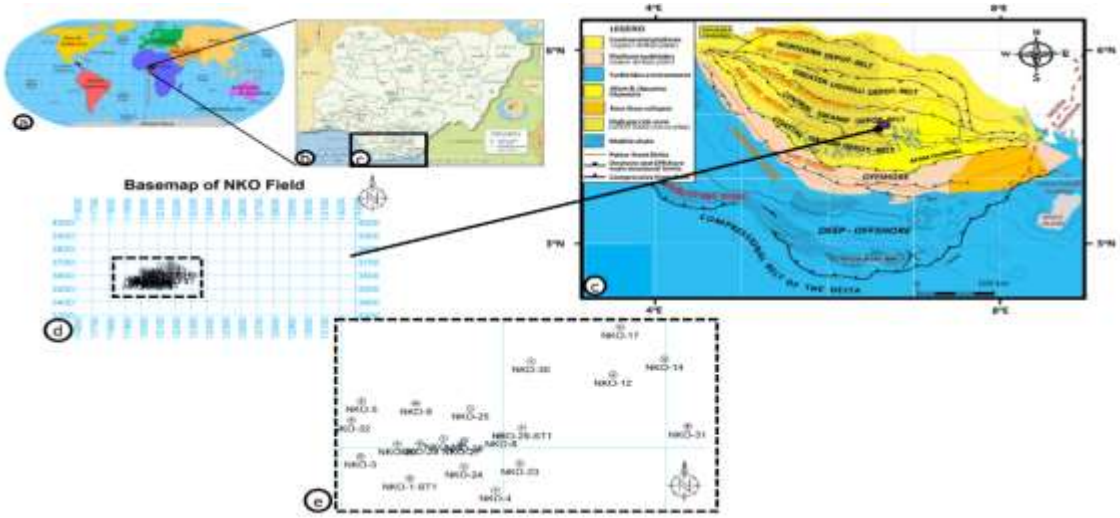

Figure 1: Location map of the study area (Nwozor et al 2013)

2.0 Materials and Methods

We analyzed well logs (GR (Gamma Ray log), DT (Sonic log), LLD & LLS (Resistivity logs), NPHI (Neutron log), and RHOB (Density log)) and the seismic data from the NKO field, focusing on reservoir_1 correlated across the wells with deeper insight on well NKO 29. Enhancing the Hydrocarbon prospect delineation of the NKO field in the Central Swamp Depobelt, Niger Delta Basin, Nigeria, will be carried out using 3-D seismic data and well logs through cross-plots and a rock physics model. The well logs and seismic data were interpreted using Schlumberger's Petrel interpretation software. Thirty-two Well-log cross-sections and corresponding seismic transects through the 3-D volume were interpreted throughout the area to present the structural framework of the Field. Petrophysical analysis will be carried out to evaluate the quality of the reservoirs and identify why there is an abrupt stop of hydrocarbon flow from the well. Well-log data for interpretation will comprise gamma-ray logs with counts measured on the horizontal scale from 0 to 150 calibrated in standard American Petroleum Institute (API). Clays contain the greatest amount of radioactive minerals, and the gamma-ray logs are primarily used in identifying clay and clay-rich facies.

Sand-rich facies also have distinctive gamma-ray signatures. A baseline of 65 API was chosen to discriminate between sand and shale. Shale has high concentrations of radioactive minerals and was delineated by GR deflection to the right (Figure 2) Interpretation of the lithologies penetrated by the studied wells within the interval of interest was determined by using a petrel calculator to set the cutoffs on the gamma-ray logs as follows: <65 API = sand, 65-80 API = silt, >80 API = shale. The well logs will be interpreted to delineate the hydrocarbon-bearing reservoirs within the study area. Well data interpretation, comprising the lithofacies analysis, reservoir identification, and fluid typing along depositional dip, will be carried out. The petrophysical parameters, Volume of Shale, Effective Porosity, Water Saturation, Net To Gross, Hydrocarbon Saturation, were determined for the identified reservoirs. A simulated seismic response computed from well data was used to correlate geological data from well-logs recorded depth (meters or feet) with geophysical data from seismic recorded time. An accurate synthetic seismogram model provided both time and depth for accurate reflection event verification and confirmation of the lithological expression of the reflection events. This is done by using check-shot data to correct the sonic log (representing velocity) multiplied by the density log to generate the acoustic impedance and reflectivity series. The reflectivity series is then convolved using a zero-phased wavelet extracted from the seismic data. The petrophysical parameters were determined for the identified reservoirs using the following relations below;

a) Volume of Shale

$$V_{sh} = \frac{GR_{log} - GR_{min}}{GR_{max} - GR_{min}} \quad (1)\ (\text{Archie, 1959})$$

Where: V_{sh} = Volume of shale, GR_{log} = Gamma ray log reading, GR_{min} = Minimum value of gamma ray reading, GR_{max} = Maximum value of gamma ray reading

b). Effective Porosity

$$\Phi_E = \Phi_T - (V_{sh} \times \Phi_T) \quad (2)\ (\text{Archie, 1959})$$

Where: Φ_E = Effective porosity, Φ_T = Total porosity, V_{sh} = Volume of shale

c) Water Saturation

$$S_w = \sqrt[n]{\frac{a \times R_W}{\Phi^m \times R_t}} \quad (3)\ (\text{Archie, 1959})$$

Where: S_W = Water saturation, n= Saturation exponent taken as 2, a= empirical constant also taken as 1, R_W = Resistivity of water formation, Φ = Porosity, m = Cementation exponent taken as 2,

R_t = True resistivity

d) Net To Gross

$$NTG = \frac{h}{H} \quad 4\ (\text{Archie, 1959})$$

Where: h = Net reservoir thickness, H = Gross reservoir thickness

e). Hydrocarbon Saturation, S_h

$$S_h = (100 - Sw)\ \% \quad (5)\ (\text{Archie, 1959})$$

Where: Sh = Hydrocarbon saturation, Sw = Water saturation

f**) Stock Tank Oil Initial In Place (STOIIP):** is calculated using equation (8) given below;

$$STOIIP = 7758 * GRV * \Phi * S_h * NTG / B_o \quad (6)$$

Where: GRV = Gross rock volume (cum), NTG = Reservoir sand Net to Gross thickness, Φ = Porosity (fractional), S_h = Hydrocarbon saturation, Bo = Oil formation volume factor, STOIIP = Stock Tank Oil Initially In Place

g) Stock Tank gas Initial In Place (STGIIP): is calculated using equation (8) given below;

GIIP = GRV *NTG* (1 – Sw)* 0.04356

STGIIP = GIIP/Bgi

Where: GRV = Gross rock volume (cum), NTG = Reservoir sand Net to Gross thickness,

S_w = water saturation, B_g = Gas formation volume factor

Gas formation volume factor can be calculated using the formula.

B_g = (0.0282*Z*T)/P where Z = Gas compressibility factor (dimensionless)

T =Température (°), P = Pressure (psi)

3.0 Results and Interpretation

3.1 Petrophysical Analysis of Well Logs for Reservoir Evaluation

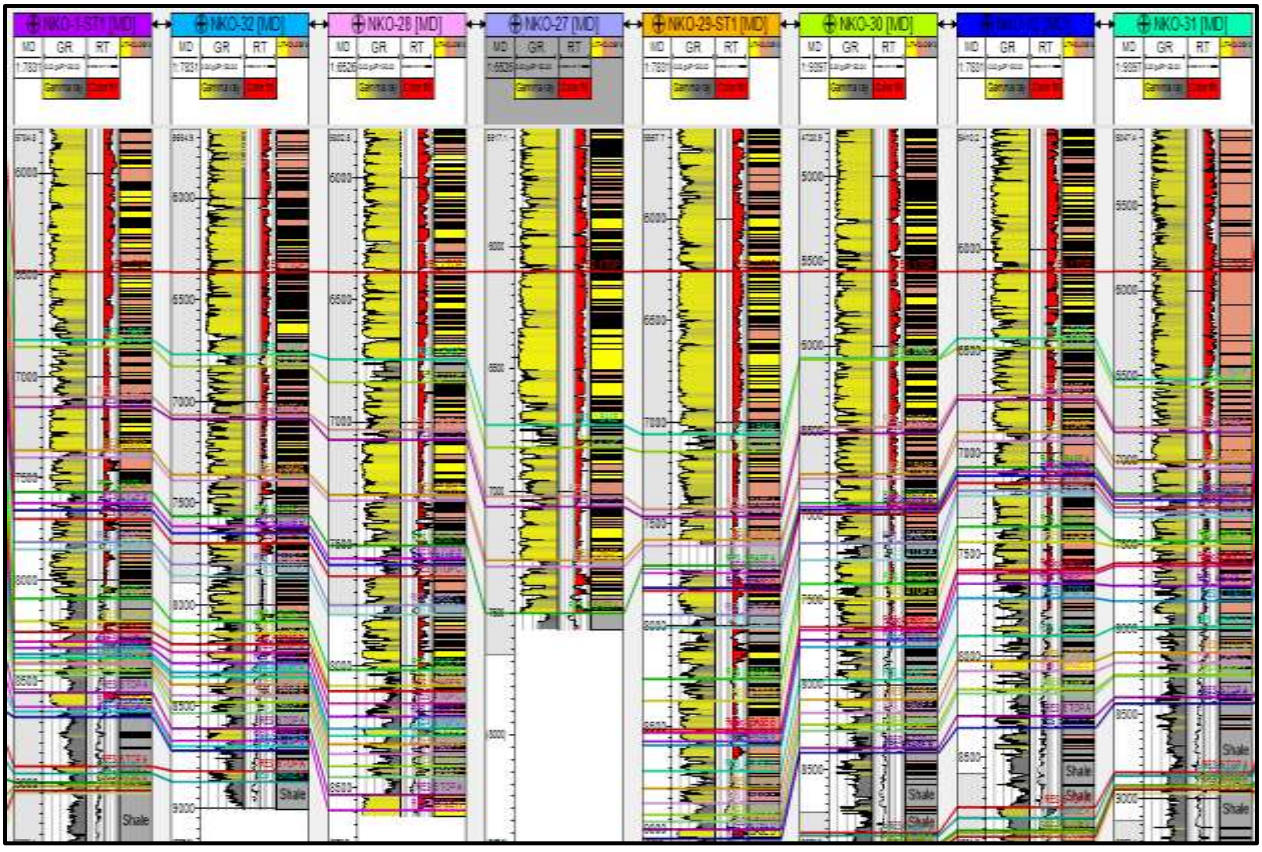

Figure 2: Well Log Correlation across the wells

The correlation of the well logs in the study area provided valuable insights into the subsurface geology, enabling a comprehensive understanding of the reservoir's structure and stratigraphy. Three distinct lithologies were identified on gamma ray log readings: shale with ≥81 API, indicating high clay content; sandstone, defined by gamma ray

readings>58 – 60 API, suggesting clean sandstones; and argillaceous sandstone, identified by gamma ray readings ≥ 65 – 69 API, indicating low clay content (Figure 2).

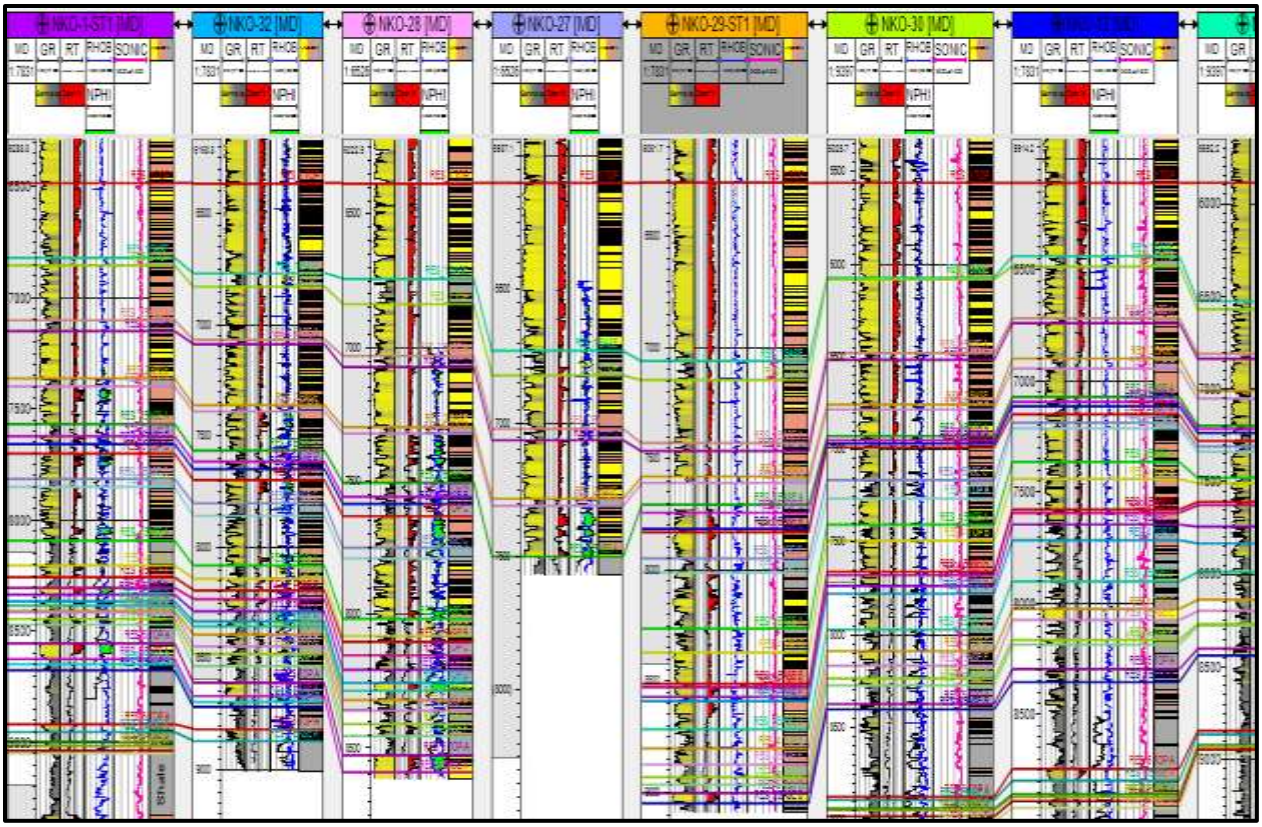

Figure 3: Well Log Analysis

Additionally, the correlation revealed evidence of structural complexity, including faults or displacement and variation in sedimentary thickness section across the wells, as shown in Figure 3. Similar lithological packages were encountered at different depth intervals in nearby wells, suggesting the presence of faults or displacement. This indicates that the reservoir has undergone tectonic activity, resulting in structural complexity. The correlated logs represent the thickest sedimentary and stratigraphically deepest section penetrated by wells within the field, providing a comprehensive understanding of the reservoir stratigraphy. Six distinct reservoirs (Res_1 to Res_6) were identified and correlated, which were further subdivided as illustrated in Figure 4 below, with focus on R_1. The delineation of these hydrocarbon-bearing sand units was facilitated by a combination of log types, enabling a detailed understanding of the reservoir architecture and potential for hydrocarbon accumulation. A comprehensive petrophysical properties analysis was performed on 32 wells to investigate the quality of the reservoir's rocks. The analysis focused on key petrophysical parameters, as volume of shale, net-to-gross volume, porosity, permeability, water saturation, and hydrocarbon saturation. These petrophysical parameters were computed using equations in the Petrel calculator, and the result of the reservoir Res_1 is summarized in Tables 1 and Figure 5.

3.2 Res_1 Reservoir Interval

The Res_1 Reservoir was successfully penetrated by all wells, exhibiting a gross thickness that varies significantly across the field, ranging from a minimum of 237 feet to a maximum of 374 feet, as clearly illustrated in Figure 5 below. The estimated average petrophysical properties of the reservoir, including porosity, permeability, and water saturation, are comprehensively depicted in Table 1 below, providing valuable insights into the reservoir's characteristics and potential hydrocarbon-bearing capabilities.

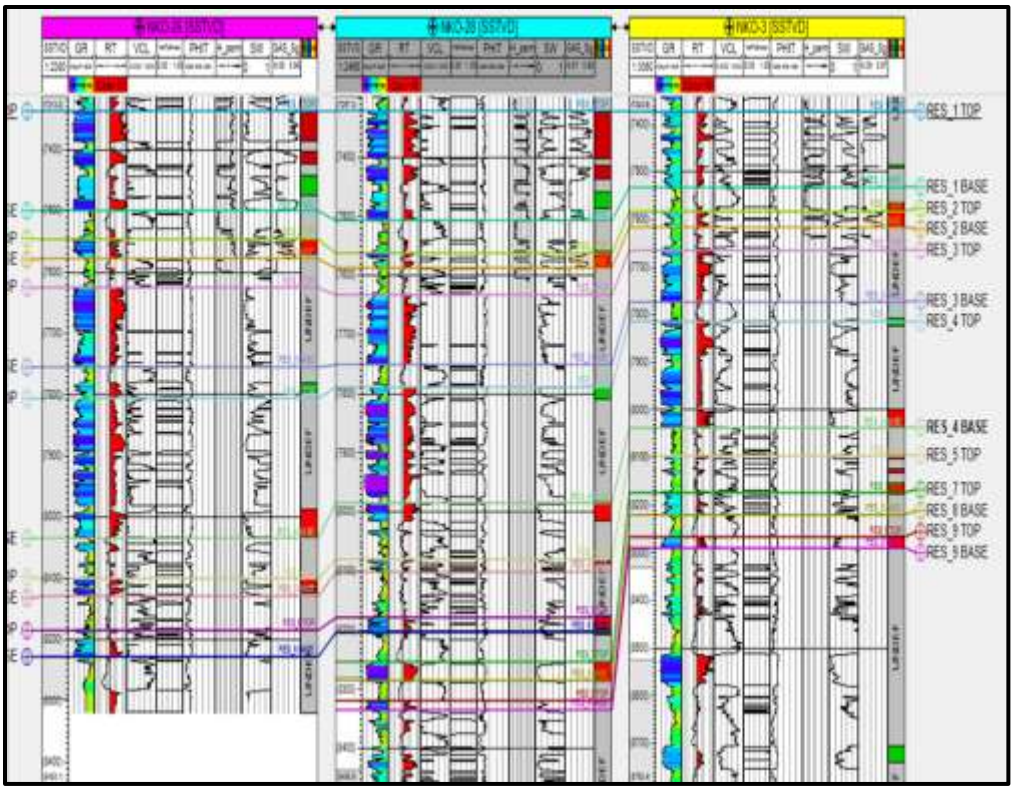

Figure 4: Showing Petrophysical Properties along The Vertical Section of the Study Area Penetrated by the Wells

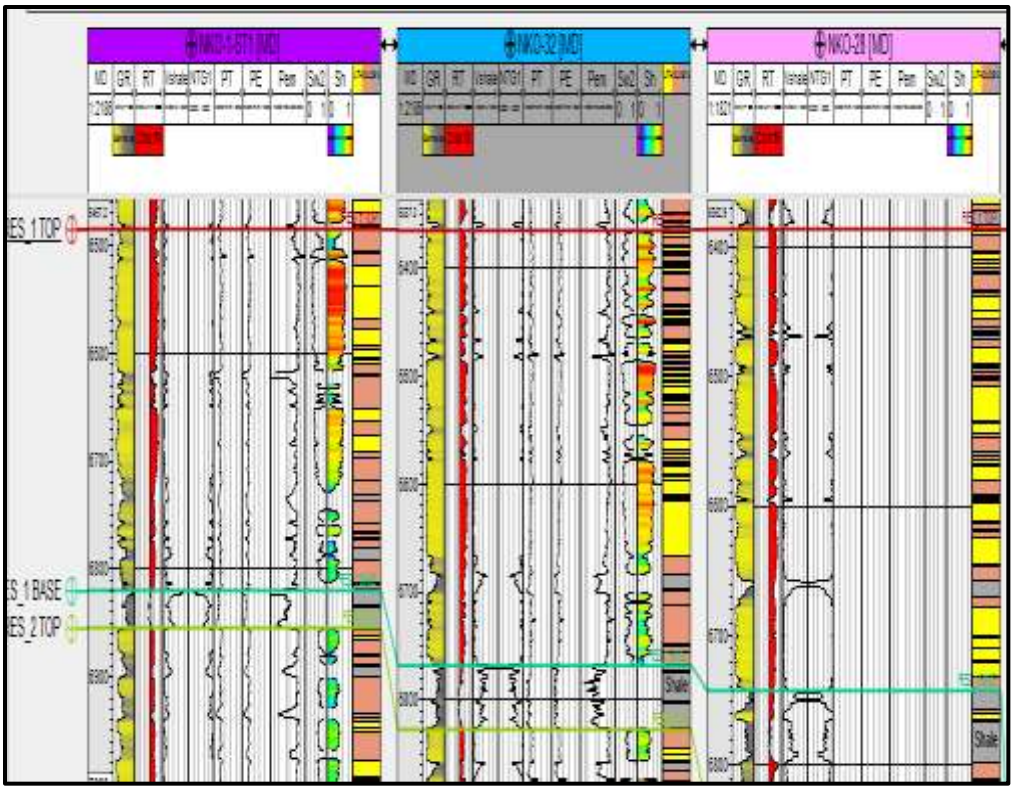

Figure 5. Res-1 Reservoir Interval Correlation across Wells

The reservoir exhibits a thinning trend towards the northeast direction, as revealed by the analysis of 32 wells. The shale volume within the reservoir ranges from 0.12 to 0.25, while the net-to-gross ratio varies between 0.75 and 0.88, indicating a relatively consistent lithology. The average effective porosity values are estimated to range from 0.20 to 0.27, suggesting moderate to good storage capacity. Permeability values, computed from relevant data, range from 541mD to 875mD, indicating a relatively high flow potential. Hydrocarbon saturation in the reservoir is found to vary between 0.56 and 0.81, which is a moderate range.

Table 1: Average Petrophysical Properties of RES_1 Reservoir Interval

Wells	V_{sh}	NTG	PE	Perm (mD)	S_h
Nko_27	0.21	0.85	0.21	751	0.81
Nko_28	0.12	0.88	0.23	823	0.74
Nko_29	0.21	0.79	0.26	798	0.84
Nok_31	0.18	0.82	0.20	652	0.56
Nko_1	0.25	0.75	0.24	741	0.62
Nko_32	0.17	0.83	0.27	658	0.71
Nko_12	0.12	0.88	0.22	547	0.68
Nko_30	0.24	0.76	0.25	875	0.65

3.3 Rock Physics

A primary objective of quantitative interpretation (QI) studies is to develop an elastic response model that effectively discriminates between various lithofacies, thereby enabling the delineation of reservoir rocks from non-reservoir intervals. Crossplots provide a valuable means of evaluating rock properties by visually illustrating the relationship between various petrophysical parameters, thereby facilitating a more insightful and meaningful analysis (Catstagna and Swan 1997). This technique enables the identification of trends, correlations, and anomalies in the data, allowing for a more nuanced understanding of the elastic properties and lithological characteristics of the reservoir.

3.4 Elastic Property Diagnostic

One of the primary objectives of a quantitative interpretation study is to model the elastic response of various lithofacies, which involves delineating reservoir and non-reservoir rocks through the use of cross-plots of different log attributes, as illustrated in Figures 6, 7, 8, and 9.

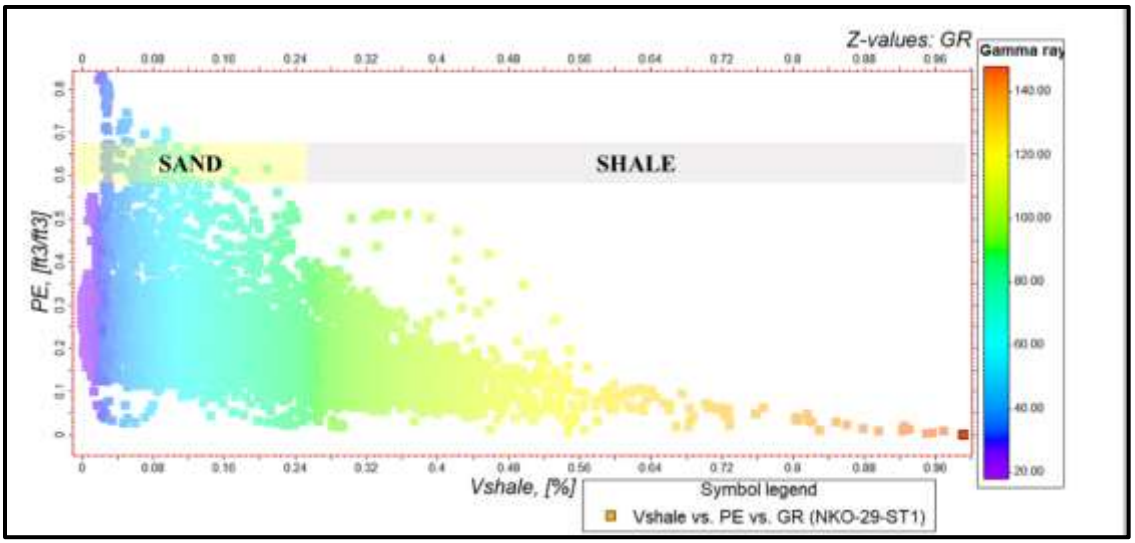

Figure 6: NKO_29-ST1 Crossplot of Effective Porosity (PE) against Volume of Shale (Vshale)

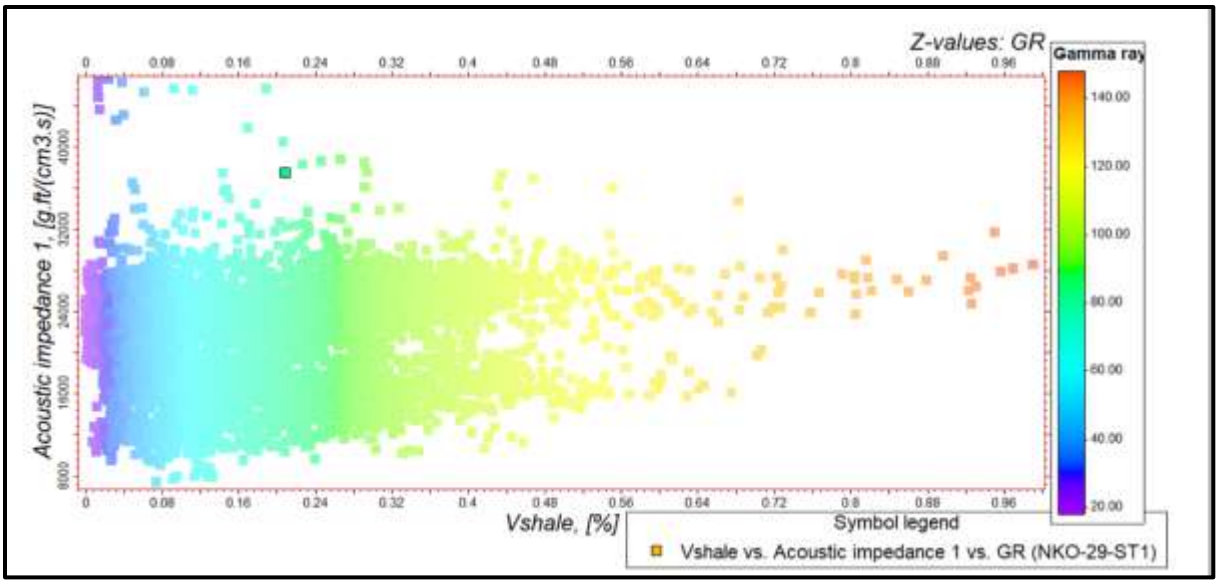

Figure 7: Well NKO_29-ST1 Crossplot of Acoustic Impedance (AI) against Volume of Shale (Vshale)

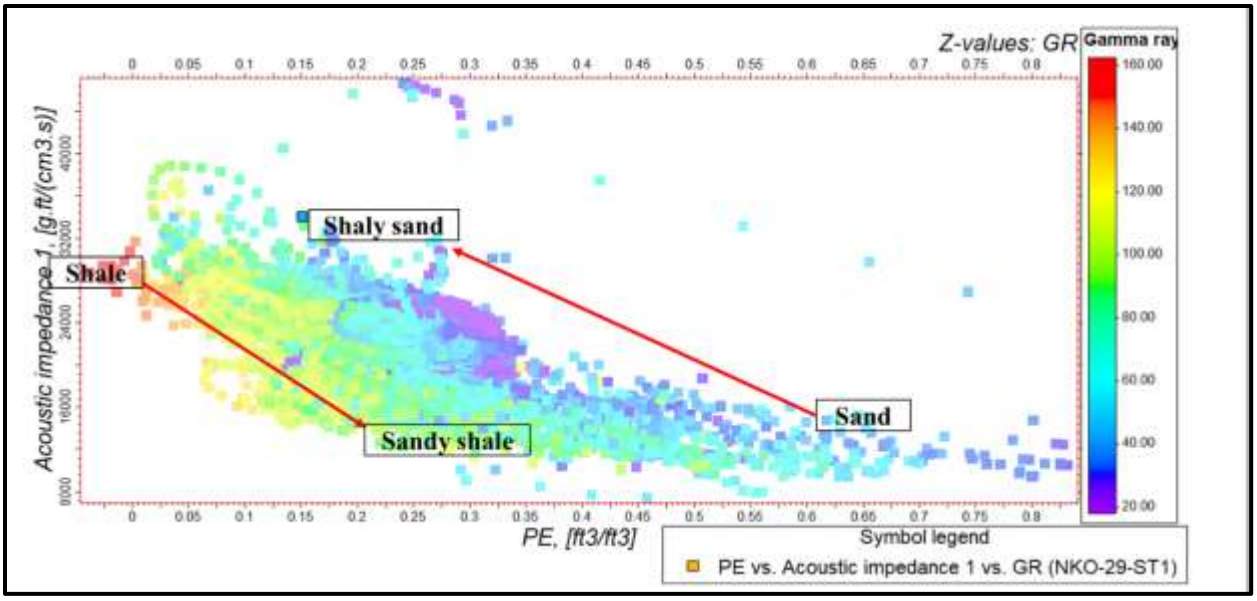

Figure 8: Well NKO_29-ST1 Crossplot of Acoustic Impedance (AI) against Effective Porosity (PE)

By leveraging the cross-plots, we were able to investigate data spread and detect elastic properties for separate facies at the same temperature and pressure conditions, thereby gaining a deeper understanding of the rock's behavior. A petro-elastic model was built using effective porosity (PE) against volume of shale (Vshale) and acoustic impedance (AI) against volume of shale, which illustrated distinct facies change from sand to shale, with the gamma ray acting as an indicator of this change, as shown in Figures 6 and 7. Analyzing the PE-Vshale relationship provided valuable insights into how elastic properties change as shale volume increases, enabling a more nuanced understanding of the rock's elastic behavior and its implications for reservoir characterization. Furthermore, a petro-elastic model of the PE-AI cross-plot, with gamma and density logs used as indicators (Figures 8 and 9), revealed a distinct shape with increasing clay content, where AI reaches its maximum and porosity reaches its minimum when clay content equals sand porosity, marking a critical transition from grain-supported sediments to clay-supported sediments. This phenomenon is pivotal in understanding the elastic behavior of rocks and has significant implications for identifying

and evaluating potential reservoir rocks, ultimately facilitating more accurate reservoir characterization and exploration.

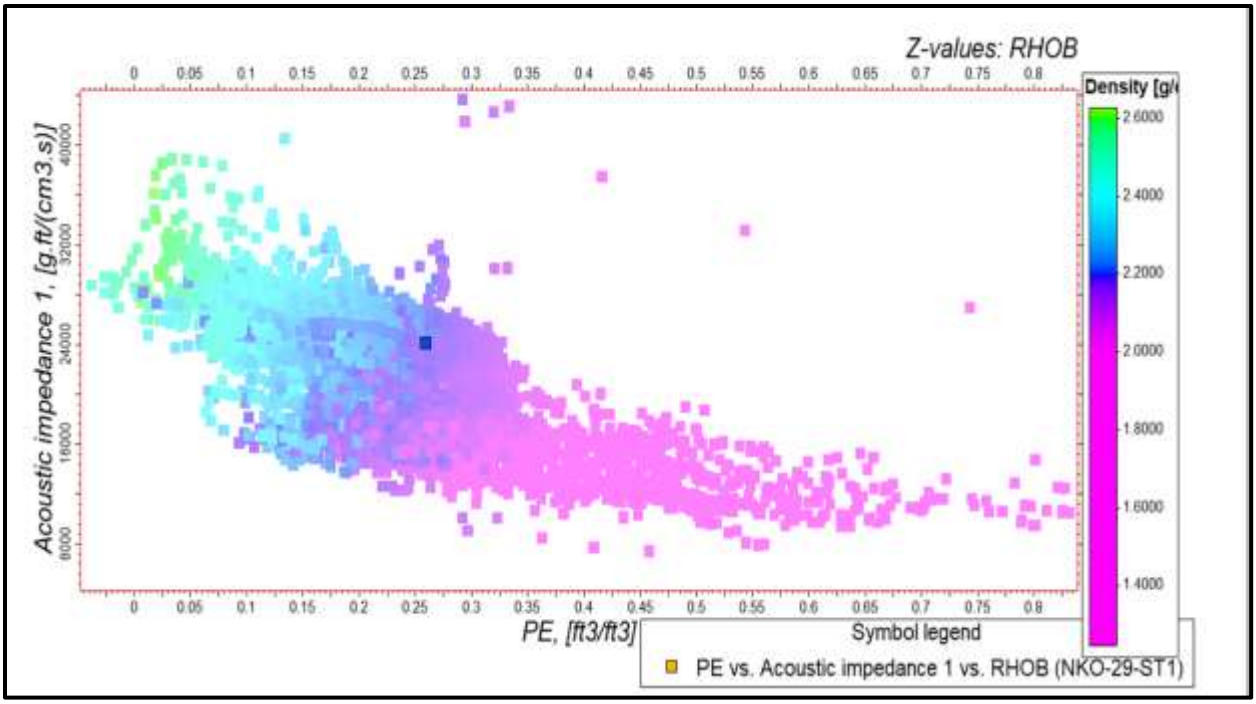

Figure 9: Well_29-ST1 Crossplot of Acoustic Impedance (AI) against Effective Porosity (PE)

3.5 Vp/VS Ratio compared to Acoustic Impedance

The velocity ratio versus P-impedance cross-plots, integrating across the reservoir in well NKO_29, distinctly delineate four primary zones: gas-bearing (red polygon), oil-bearing (yellow polygon), brine-bearing (blue polygon), and shaly intervals (purple polygon) as shown in Figure 10. A notable observation in mixed hydrocarbon-brine reservoirs is the significantly lower velocity ratio values exhibited by hydrocarbon-bearing sands compared to their brine-filled counterparts. This disparity stems from the inherent sensitivity of P-waves to fluid changes, whereas S-waves remain relatively insensitive (Han et al. 2007; Ujuanbi et al. 2008; Krebs et al. 2009; Ogararue and Anine 2016). Consequently, the velocity ratio serves as a reliable fluid indicator. The cross-plot analysis presented in Figure 10 effectively resolves the fluid lithology types encountered by the well, underscoring the diagnostic capability of this approach. A reduction in velocity ratio is anticipated when transitioning from brine to oil or from oil to gas, highlighting the potential for fluid discrimination. Furthermore, P-impedance, being the product of P-wave velocity and density, exhibits a compounded effect in distinguishing hydrocarbon-bearing sands from brine-filled sands. As both P-wave velocity and density respond similarly to hydrocarbon presence with a reduction in values, their product (P-impedance) is expected to accentuate the differentiation under normal conditions, thereby enhancing the identification of hydrocarbon-bearing intervals.

3.6 Reservoirs upscale

Upscaling of well logs was conducted to populate the 3D grid with petrophysical and facies properties. The upscaling involved selecting wells with relevant log data and with the volume of shale designated as the first property to undergo this process. The upscaling methodology was defined by the following parameters: The arithmetic algorithm being employed for upscaling, treating logs as lines, and utilizing the simple cells method to capture local variations. This average approach enabled the calculation of the averaged log values for each 3D grid cell penetrated by the wells. The upscaling process was systematically applied to various petrophysical properties, including: net-to-gross ratio, porosity, permeability, water saturation, hydrocarbon saturation, and facies. For each of the cells intersected by the well, the log values within that cell were averaged according to the selected algorithm, resulting in a single representative value for the cell. The resulting 3D contained populated values only for the cells penetrated by wells, providing a detailed and accurate representation of the reservoir's petrophysical properties. Upscaling aimed to

enhance production potentials, efficiency, or recovery factor of the reservoir, and also the values of each petrophysical parameter in the geocell designed in its geometrical location. The two primary conditions for upscaling are that the data has a normal distribution and that the input values have no specific orientation. The upscaling accurately presented the geological features and properties of reservoirs in the NKO Field, such as heterogeneity, faults, and fractured zones. It equally captured the flow behavior of fluid in the reservoir, including multiphase flow, viscosity, and relative permeability.

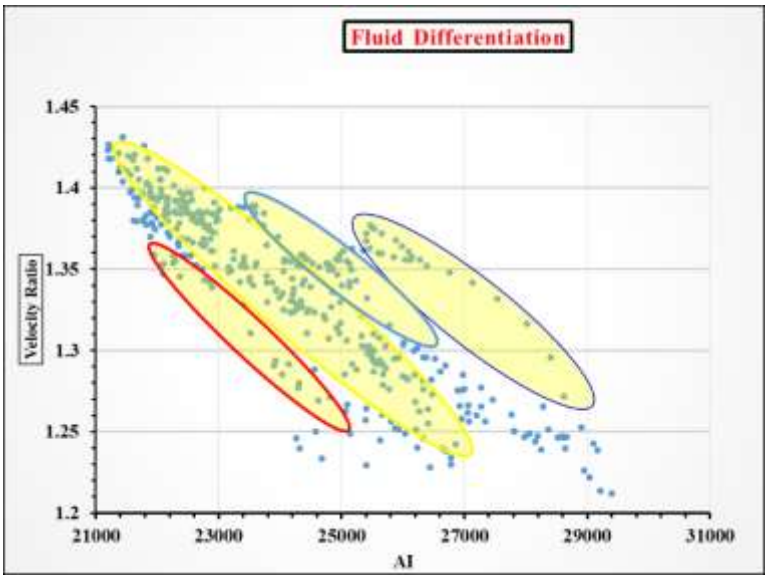

Figure 10: Crossplot of Velocity Ratio versus Acoustic Impedance for well NKO_29-ST1

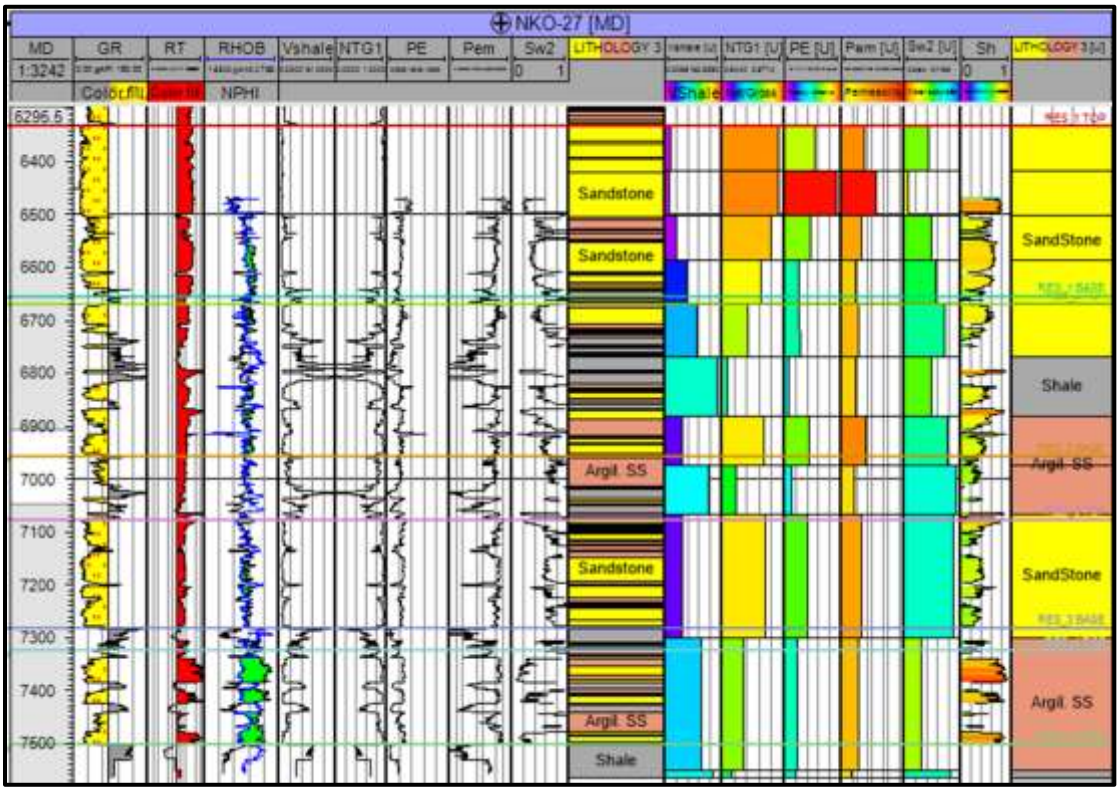

Figure 11: Showing the Upscale Well Logs for Well NKO_27

3.7 Facies Modeling

The initial stage of facies modeling involved creating discrete facies that were upscaled to grid-based model cells, as illustrated in Figure 11. This process enabled the integration of geological and petrophysical data. The Res_1 reservoir surface exhibited intercalation of sands and shale, which were analyzed and quantified through comprehensive data analysis. The interpreted facies of the reservoir surfaces comprise sandstone (yellow), argillaceous sandstone (orange-pink), and shale (gray); these indicate that the facies were deposited in a fluctuating regime ranging from lower intertidal to slightly deep subtidal environments. The spatial distribution shows sandstone-dominated regions interspersed with shale and argillaceous sands. These patterns suggest fluvial or deltaic deposition, which is consistent with high reservoir heterogeneity. Zones dominated by yellow (sandstone) are the most prospective due to their higher porosity and permeability (Figure 12).

However, the thickness-frequency histogram further supports the heterogeneity of the system (Figure 13). Most lithological units are less than 400 ft. thick, indicating thin but laterally extensive layers, characteristic of fluvial deposits. While sandstone dominates the thinner intervals, shale is more evenly distributed across various thicknesses, suggesting background or mass deposition or interbedding. A cross-section of the reservoirs shown in both Figure 12 and Figure 13 shows the lateral and vertical changes of facies. The rapid changes across the studied wells reflect changes in depositional conditions, underscoring the complexity of the reservoir's geological architecture.

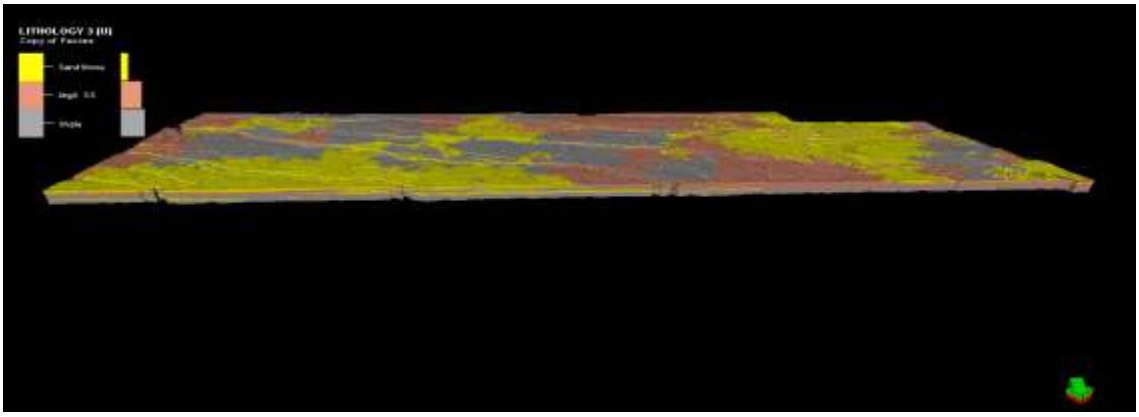

Figure 12: Facies Analysis for the Six Reservoir Surfaces

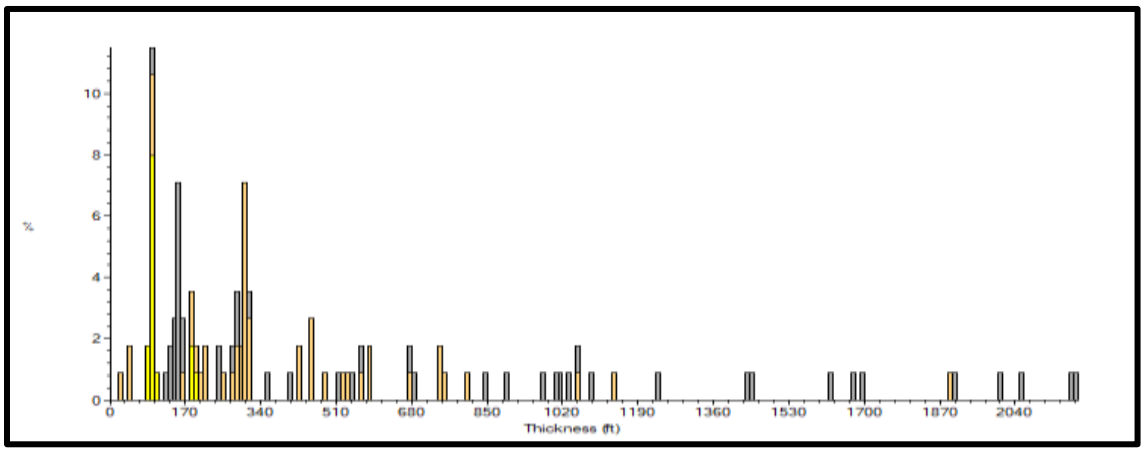

Figure 13: Histogram Analysis for Six Reservoir Surfaces

3.8 Petrophysical/ Property Modeling

Following the upscaled value of the reservoir petrophysical properties, the sequential Gaussian simulation (SGS) algorithm was employed as the statistical approach for petrophysical modeling. Given the available data, SGS proved to be the most suitable method, offering an advantage in simulating continuous variables such as volume of shale, net-to-gross, porosity, permeability, water saturation, and hydrocarbon saturation. The SGS process involved determining

parameter values for unsampled intervals using equations derived from data regression. Normal scoring was applied to ensure that all values satisfied the normal distribution. The petrophysical model of the NKO field reservoirs revealed the following trends:

3.8.1 *Volume of shale*

The volume of shale for the NKO field indicates an estimate of 0.00 to 100 percent at the well location. This indicates a good, productive zone with clean sand distribution.

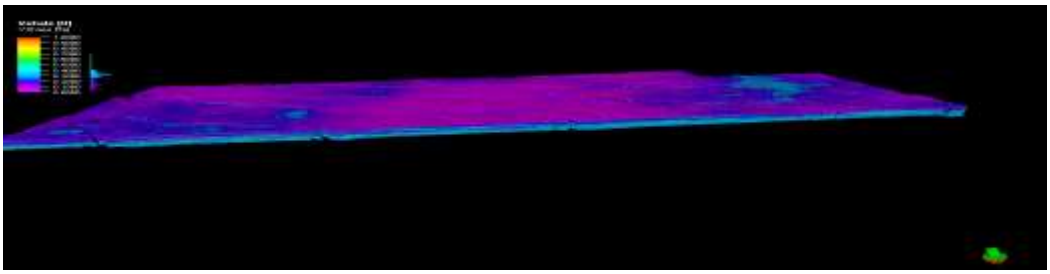

Figure 14: Volume of Shale for the Six Reservoir Surfaces

3.8.2 *Net-To-Gross*

Net-to-gross estimates range from 00-100 percent. This indicates a relatively large hydrocarbon zone when compared with the shale fraction.

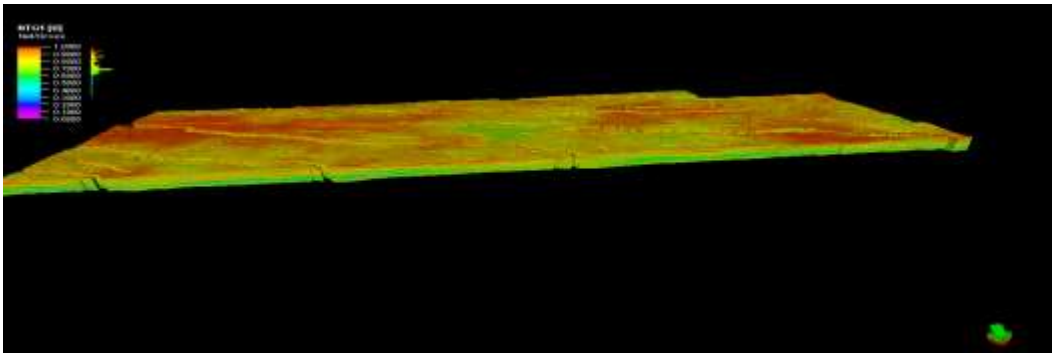

Figure 15: Net-To-Gross Model for the Reservoir Surfaces

3.8.3 *Effective Porosity*

Investigation of the porosity model revealed a range of porosity between 0.00 and 50 percent for the NKO field. These values indicate possible hydrocarbon pore volume with well-interconnected pore spaces and water-wet reservoir rocks, which permit high reservoir deliverability.

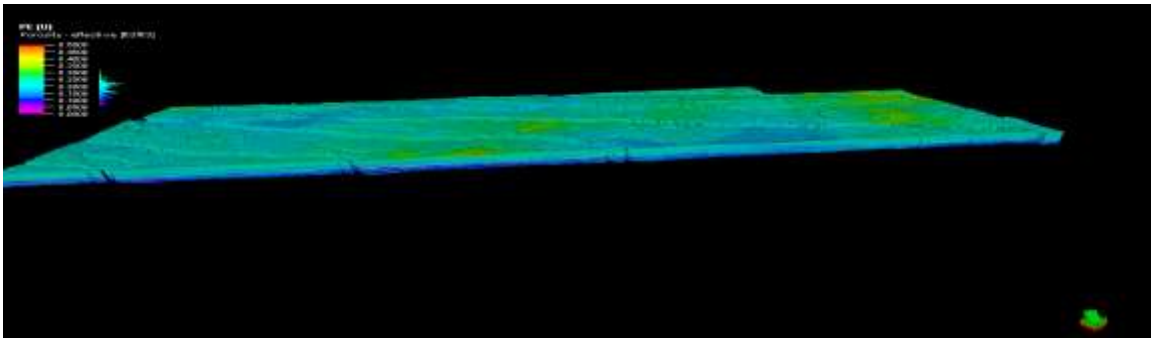

Figure 16: Effective Porosity Model for the Six Reservoir Surfaces

3.8.4 *Permeability*

Investigation of the permeability model revealed reservoir permeability of 0.1 to 1000mD at well locations. At the north-east location of the wells, permeability is high between 100 and 1000mD. With good hydrocarbon pore volume, high reservoir deliverability is expected within the producing zone of the reservoir.

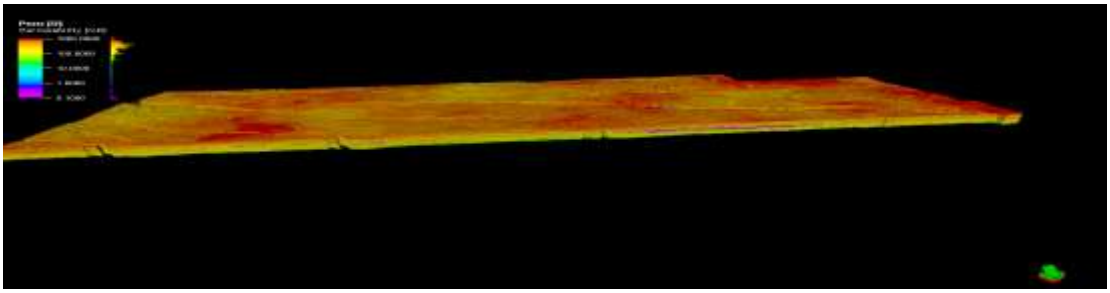

Figure 17: Permeability Model for the Six Reservoir Surfaces

3.8.5 *Water Saturation Model*

Facies distribution also offers an indication of the distribution of water saturation, which enabled building a model for water saturation for each reservoir unit within the study area. The water saturation value ranges from 0.00 to 1.00, as shown in the figure below.

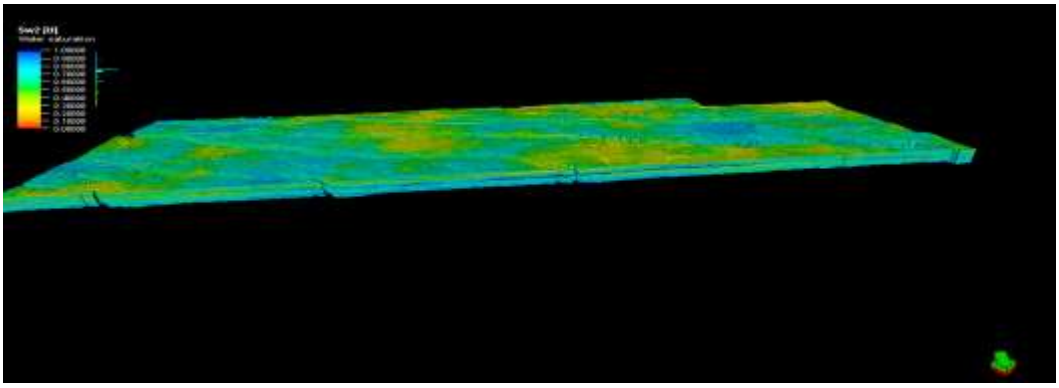

Figure 18: Water Saturation Model for the Six Reservoir Surfaces

3.8.6 *Hydrocarbon Saturation*

Facies distribution also offers an indication of the distribution of hydrocarbon saturation that enabled the building of a model for hydrocarbon saturation for each reservoir unit within the study area. The hydrocarbon saturation ranges from 0.00 to 1.00 as shown in the figure below.

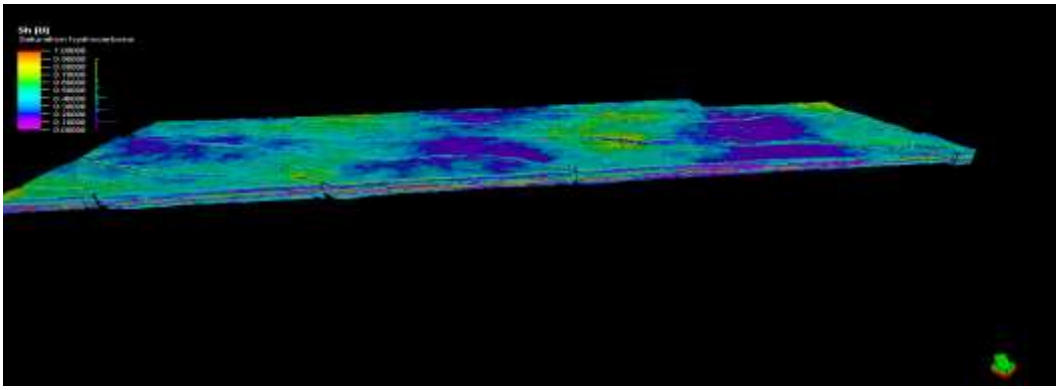

Figure 19: Hydrocarbon Saturation Model for the Six Reservoir Surfaces

3.8.7 *Fluid Contacts*

Figure 20: Fluid Contacts Model for the Six Reservoirs

The model indicated that the zones exhibit good to very good reservoir quality. That is high porosity and permeability values, and low water saturation, particularly in intervals with sandy facies.

3.9 Volumetrics

For a realistic resource estimation, volumetric calculation was employed in conjunction with a geological reservoir model. The volumetric estimation of both oil and gas in place within the NKO Field reservoir was performed using the 3D grid-based geo-model. The parameters used in the calculation are based on the cellular model developed earlier in this work. The estimated Stock Tank Oil Initially Place (STOIIP) and Stock Tank Gas Initially Place (STGIIP) of reservoir 1 at NKO field were assessed to be approximately 102,926,142.7 stock tank barrels of oil and 1,112,563,192 standard cubic feet of gas, respectively, with an estimated gas formation volume factor (B_g) of 100%. This volumetric calculation provides a quantitative estimate of hydrocarbon resources in place, serving as a critical input for reservoir characterization, development planning, and production forecasting.

Table 2: Volumetrics for the Reservoir 1

Zone/Reservoir	Bulk volume [bbl]	Net volume [bbl]	Pore volume [RB]	HCPV oil [RB]	STOIIP (in oil) [STB]	Recoverable [STB]
Res_1 Depth	3995580075	$3.876*10^9$	882224080.6	529334448.3	294074693.5	102,926,142.7

Table 3: Volumetrics for the Gas in Reservoir 1 with 100% recovery factor

Zones	Bulk volume[bbl]	Net volume [bbl]	Pore volume [RB]	HCPV gas [RB]	GIIP (in gas) [MSCF]	STGIIP [MSCF]	Recoverable gas [MSCF]
Res_1 Interval	8397970951	$7.726 * 10^9$	1854271986	1112563192	1112563192	1112563192	1,112,563,192

4.0 Conclusion

This study has successfully demonstrated the effectiveness of the rock physics model in comprehensive reservoir characterization for enhanced hydrocarbon prospect delineation in the NKO field, Niger Delta Basin. A petro-elastic model was developed to discriminate between lithofacies, enabling the delineation of reservoir rocks from non-reservoir intervals. Cross-plots of log attributes, such as PE-Vshale and AI-Vshale, revealed distinct facies changes from sand to shale, providing valuable insights into elastic properties and lithological characteristics. Velocity ratio versus P-impedance cross-plots effectively discriminated fluid types and lithologies, identifying four primary zones: gas-bearing, oil-bearing, brine-bearing, and shaly intervals. Furthermore, the velocity ratio's sensitivity to fluid changes and P-impedance's ability to accentuate differences between hydrocarbon-bearing and brine-filled sands make this approach a reliable tool for identifying hydrocarbon-bearing intervals.

The volumetric calculation of hydrocarbon resources provided a robust estimate of oil and gas in place, with an estimated STOIIP and STGIIP at the NKO field, which was assessed to be approximately 102926142.7 stock tank barrels with an estimated recovery factor of 35% and 1112563192 standard cubic feet with an estimated recovery factor of 100% approximately. This quantitative assessment serves as a critical foundation for reservoir characterization, development planning, and production forecasting, ultimately informing strategic decisions for optimal field development and resource extraction.

These research findings will be useful in the petroleum industry by increasing the hydrocarbon reserve within the Niger Delta Basin, which will translate into increased energy resources for Nigeria. It will also enhance the understanding of the various play elements' nature, configuration, and viability for brownfield development. Again, it will be very useful for the academic research community as it provides a better workflow for integrated reservoir characterization and reassessing old producing fields within the basin and globally.

5.0 Recommendation

To gain a more comprehensive understanding of the reservoirs and accurately interpret the depositional environments, it is recommended that geochemical, biostratigraphy, and seismic inversion studies be employed. These integrated studies will provide valuable insights into the reservoir's characteristics, enabling a more reliable interpretation of the subsurface geology.

References

Allo, O.J., Ayolabi, E., A, Adeoti, L.,Akinmosin, A., Oladele, S.2022. Reservoir characterization for hydrocarbon detection using Amplitude Variation with Angles constrained by localized rock physics template. Journal of African Earth Sciences, doi: 10.1016/j.jafrearsci.2022.104548

Castagna, J.P., and Swan, H.W.1997. Principles of AVO Cross Plotting. The Leading Edge, 6, 337-344.

Chris, Carpenter. 2022. Rock Physics Model Provides Insight into Reservoir Characterization. Journal of Petroleum Technology, doi: 10.2118/0222-0078-jpt

Goodway, W., Chen, T., Downton, J. 1997. improved AVO fluid detection and lithology discrimination using lame petrophysical parameters. The Society of Exploration Geophysicists. In: 67th annual international meeting, Denver.

Han, D.H., Yao, Q., Zhao, H.Z 2007. Complex properties of heavy oil sand:77th annual international meeting of SEG expanded abstract, vol 77, p. 1609-1613. DOI: 10.1190/1.2792803

Krebs, J.R., Anderson, J.E., Hinkley, D., Neelamani, R., Lee, S., Baumstein, A., Lacasses, M.D. 2009. Fast full-wave field seismic inversion using encoded sources. Geophysics 74(6):177-188. DOI: 10.1190/1.3230502

Nakajigo, J., Kiberu, J.M., Johansen, T.A., Jensen, E.H., John, V., Tiberindwa. 2023. Rock physics analysis of reservoir units of the Semliki basin, Albertine graben: A case study. Journal of African Earth Sciences, doi: 10.1016/j.jafrearsci.2023.104876

Nwozor, K. R., Omudu M. I., Ozumba B. M., Egbuachor, C. J., Onwumesi, A. G., and Anike O. L., 2013. Quantitative evidence of secondary mechanisms of over pressure generation: Insights from parts of onshore Niger Delta, Nigeria, Journal of Petroleum Technology Development, 3 (1), 64-83

Ogararue, D.O. and Anine, D.O. 2016. An integration of rock physics, AVO modelling, and analysis for reservoir fluid and lithology determination in a Niger Delta deep water block. IOSR J Appl Geol Geophys 4:36-46

Pickett, G. (1963). Acoustic character logs and their applications: information evaluation. J Pet Technol 15:650-667

Triveni, Gogoi, and Rima, Chatterjee.. 2021. An integrated petrophysical and rock physics analysis for a reservoir characterization study in parts of the Upper Assam basin, India. Arabian Journal of Geosciences, doi: 10.1007/S12517-021-08240-7

Ujuanbi,O., Okolie, J.C. and Jegede, S.I. 2008 Lambda-Mu-Rho techniques as a variable tool for litho-fluid discrimination – the Niger Delta example: International of Physical Sciences, v. 2/7, p. 173-176.